EPJ Web of Conferences **81**, 01007 (2014)
DOI: 10.1051/epjconf/20148101007

Single and double charmed meson production at the LHC

Rafal Maciula[1, a] and Antoni Szczurek[1,2]

[1] *Institute of Nuclear Physics PAN, PL-31-342 Cracow, Poland*
[2] *University of Rzeszów, PL-35-959 Rzeszów, Poland*

Abstract. We discuss production of charmed mesons in proton-proton collisions at the LHC. The cross section for inclusive production of $c\bar{c}$ pairs is calculated in the framework of the $k_{\perp}$-factorization approach which effectively includes next-to-leading order corrections. Theoretical uncertainties of the model related to the choice of renormalization and factorization scales as well as due to the quark mass are discussed. Results of the $k_{\perp}$-factorization approach are compared to NLO parton model predictions. The hadronization of charm quarks is included with the help of the Peterson fragmentation functions. Inclusive differential distributions in transverse momentum for several charmed mesons (D^0, $D^{\pm}$, $D_S^{\pm}$) are calculated and compared to recent results of the ALICE, ATLAS and LHCb collaborations. Furthermore, we also discuss production of two pairs of $c\bar{c}$ within a simple formalism of double-parton scattering (DPS). Surprisingly large cross sections, comparable to single-parton scattering (SPS) contribution, are predicted for LHC energies. We compare our predictions for double charm production (DD meson-meson pairs) with recent results of the LHCb collaboration for azimuthal angle φ_{DD} and rapidity distance between mesons Y_{DD}. Meson-meson kinematical correlations are also confronted with those related to the standard meson-antimeson measurements. Our calculations clearly confirm the dominance of DPS in the production of events with double charm, however some strength seems to be still lacking. Possible missing contribution within the framework of single-ladder-splitting DPS mechanism is also discussed.

1 Introduction

Recently, ATLAS [1], ALICE [2, 3] and LHCb [4] collaborations have measured inclusive distributions for different charmed mesons. The LHCb collaboration has measured in addition a few correlation observables for charmed meson-antimeson pairs in the forward region $2 < y < 4$ [5].

Commonly in the exploration of heavy quark production the main efforts concentrate on inclusive distributions. Improved schemes of standrad pQCD NLO collinear approach are state of art in this respect. On the other hand, the k_t-factorization approach is commonly used as a very efficient tool for more exclusive studies of kinematical correlations (see e.g. [6] and references therein). In this approach the transverse momenta of incident partons are explicitly taken into account and their emission is encoded in the unintegrated gluon distributions (UGDFs). This allows to construct different correlation distributions which are strictly related to the transverse momenta of initial particles.

a. e-mail: rafal.maciula@ifj.edu.pl

It was argued recently that the cross section for $c\bar{c}c\bar{c}$ production at the LHC may be very large due to mechanism of double-parton scattering (DPS) [7]. In the meanwhile the LHCb collaboration measured the cross section for the production of DD meson-meson pairs at $\sqrt{s}$ = 7 TeV which is surprisingly large, including interesting correlation distributions [5]. So far those data sets for double open charm production have been studied differentially only within the $k_{\perp}$-factorization approach using unintegrated gluon distributions [8], where several observables useful to identify the DPS effects in the case of double open charm production have been carefully discussed. In order to draw definite conclusions about the DPS effects in double charm production it is necessary to estimate contribution to $c\bar{c}c\bar{c}$ final state from the standard mechanism of single-parton scattering [9].

2 Single charmed meson production

The cross section for the production of a pair of charm quark – charm antiquark within the k_t-factorization approach can be written as:

$$\frac{d\sigma(pp \to c\bar{c}X)}{dy_1 dy_2 d^2p_{1t} d^2p_{2t}} = \frac{1}{16\pi^2 \hat{s}^2} \int \frac{d^2k_{1t}}{\pi} \frac{d^2k_{2t}}{\pi} \overline{|\mathcal{M}^{off}_{g^*g^* \to c\,\bar{c}}|^2} \times \delta^2\left(\vec{k}_{1t} + \vec{k}_{2t} - \vec{p}_{1t} - \vec{p}_{2t}\right) \mathcal{F}_g(x_1, k_{1t}^2, \mu^2) \mathcal{F}_g(x_2, k_{2t}^2, \mu^2). \tag{1}$$

The crucial ingredients in the formula above are off-shell matrix elements for $g^*g^* \to c\,\bar{c}$ subprocess and unintegrated (transverse momentum dependent) gluon distributions (UGDF). The relevent matrix elements are known and can be found, e.g in Ref. [10]. The unintegrated gluon distributions are functions of longitudinal momentum fraction x_1 or x_2 of gluon with respect to its parent nucleon and of gluon transverse momenta k_t. Some of them depend in addition on the factorization scale μ.

Several UGDFs have been discussed in the literature. In contrast to the collinear gluon distributions (PDFs) they differ considerably among themselves. One may expect that they will lead to different production rates of $c\bar{c}$ pairs at the LHC. Since the production of charm quarks is known to be dominated by the gluon-gluon fusion, the charm production in hadronic reactions at the LHC can be used to verify the quite different models of UGDFs in an unique kinematical and dynamical domain.

The hadronization of heavy quarks is usually done with the help of fragmentation functions. The inclusive distributions of charmed mesons can be obtained through a convolution of inclusive distributions of charm quarks/antiquarks and $c \to$ D fragmentation functions:

$$\frac{d\sigma(pp \to DX)}{dy_D d^2p_{t,D}} \approx \int_0^1 \frac{dz}{z^2} D_{c\to D}(z) \frac{d\sigma(pp \to c\bar{c}X)}{dy_c d^2p_{t,c}}\Bigg|_{\substack{y_c = y_D \\ p_{t,c} = p_{t,D}/z}}, \tag{2}$$

where $p_{t,c} = \frac{p_{t,D}}{z}$ and z is the fraction of longitudinal momentum of heavy quark carried by meson. In our calculations we use standard Peterson model of fragmentation function [11], normalized to the proper branching fractions from Ref. [12].

In Fig. 1 we show transverse momentum distribution of D^0 mesons. In the left panel we present results for different UGDFs known from the literature. Most of the UGDFs applied here fail to describe the ALICE data. The KMR UGDF [13] provides the best description of the measured distributions. Therefore in the following we shall concentrate only on the calculations based on the KMR UGDF. In the right panel we have presented the uncertainties coming from the perturbative part of the calculation. The uncertainties of our predictions are obtained by changing charm quark mass $m_c = 1.5 \pm 0.3$ GeV and by varying renormalization and factorization scales $\mu^2 = \zeta m_t^2$, where $\zeta \in (0.5; 2)$. The gray shaded bands represent these both sources of uncertainties summed in quadrature. In addition, the results of relevant calculations within the LO and NLO collinear approach are presented for comparison. The k_t-factorization approach with the KMR UGDF is consistent with the NLO collinear calculations.

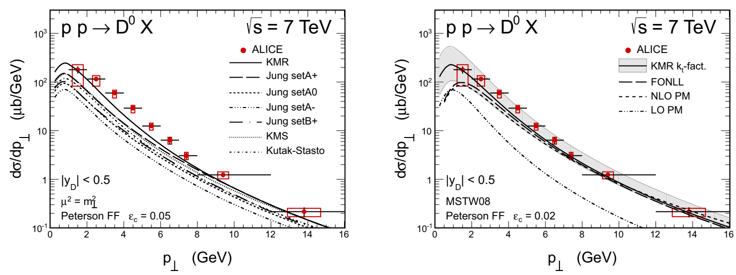

Figure 1. Transverse momentum distribution of D^0 meson for different UGDFs (left) and for the KMR UGDF compared to the pQCD collinear calculations (right) together with the ALICE data. Details of the calculations are specified in the figure.

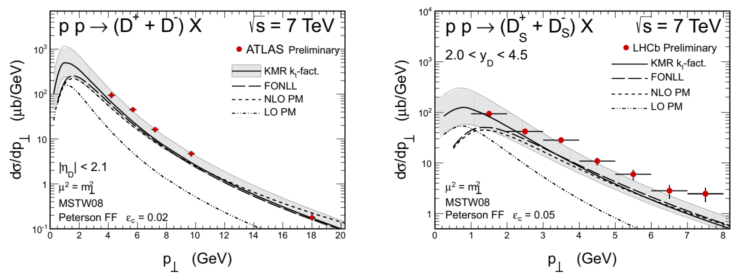

Figure 2. Transverse momentum distribution of $D^{\pm}$ meson for the ATLAS experiment (left) and transverse momentum distribution of $D_S^{\pm}$ for the LHCb experiment (right). Together with our predictions for the KMR UGDF (solid line with shaded band). Results of pQCD collinear approaches are also shown.

The left panel of Fig. 2 shows transverse momentum distributions of charged pseudoscalar $D^{\pm}$ mesons measured by the ATLAS experiment. Overall situation is very similar as for the ALICE case except of the agreement with the experimental data points, which is somewhat worse here. Only the very upper limit of the KMR result is consistent with the ATLAS data. This is also true for the other standard collinear NLO pQCD approaches. The worse description of the ATLAS data may be caused by much broader range of pseudorapidities than in the case of the ALICE detector. Potentially, this can be related to double-parton scattering (DPS) effects [8].

Recently the LHCb collaboration presented first results for the production of different D mesons in in the forward rapidity region $2 < y < 4.5$. In this case one can test asymmetric configuration of gluon longitudinal momentum fractions: $x_1 \sim 10^{-5}$ and $x_2 > 10^{-2}$. Standard collinear gluon distributions as well as unintegrated ones were never tested at such small values of x. In the right panel of Fig. 2 we present transverse momentum distribution for $D_s^{\pm}$ meson. The main conclusions are the same as for ALICE and ATLAS conditions. Our results with the KMR UGDF within uncertainties are consistent (with respect to the upper limits) with the experimental data and with the NLO collinear predictions.

3 Double open charm at the LHC

Production of double charm ($c\bar{c}c\bar{c}$ four-parton final state) is particularly interesting especially in the context of experiments being carried out at the LHC and has been recently carefully discussed [7, 8]. The double-parton scattering formalism in the simplest form assumes two independent standard single-parton scatterings (see left diagram of Fig. 3). Then in a simple probabilistic picture, in the so-called factorized Ansatz, the differential cross section for DPS production of $c\bar{c}c\bar{c}$ system within the

$k_\perp$-factorization approach can be written as:

$$\frac{d\sigma^{DPS}(pp \to c\bar{c}c\bar{c}X)}{dy_1 dy_2 d^2p_{1,t} d^2p_{2,t} dy_3 dy_4 d^2p_{3,t} d^2p_{4,t}} = \frac{1}{2\sigma_{eff}} \cdot \frac{d\sigma^{SPS}(pp \to c\bar{c}X_1)}{dy_1 dy_2 d^2p_{1,t} d^2p_{2,t}} \cdot \frac{d\sigma^{SPS}(pp \to c\bar{c}X_2)}{dy_3 dy_4 d^2p_{3,t} d^2p_{4,t}}. \quad (3)$$

When integrating over kinematical variables one obtains

$$\sigma^{DPS}(pp \to c\bar{c}c\bar{c}X) = \frac{1}{2\sigma_{eff}} \sigma^{SPS}(pp \to c\bar{c}X_1) \cdot \sigma^{SPS}(pp \to c\bar{c}X_2). \quad (4)$$

These formulae assume that the two partonic subprocesses are not correlated one with each other and do not interfere. The parameter σ_{eff} in the denominator of the above formulae from a phenomenological point of view is a non-perturbative quantity related to the transverse size of the hadrons and has the dimension of a cross section. The dependence of σ_{eff} on the total energy at fixed scales is rather small and it is believed, that the value should be equal to the total non-diffractive cross section, if the hard-scatterings are really uncorrelated. More details of the theoretical framework for DPS mechanism applied here can be found in Ref. [8].

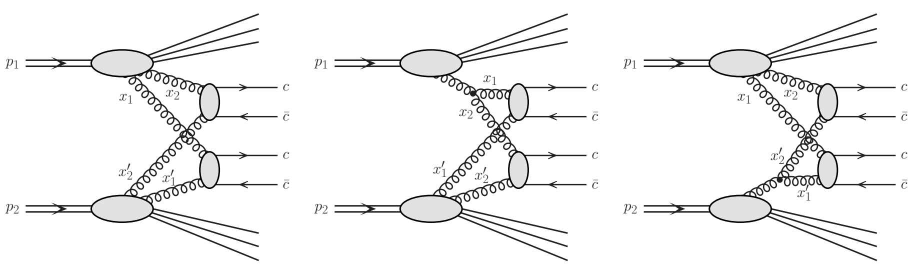

Figure 3. The standard (left) and single-ladder-splitting (middle and right) diagrams for DPS production of $c\bar{c}c\bar{c}$.

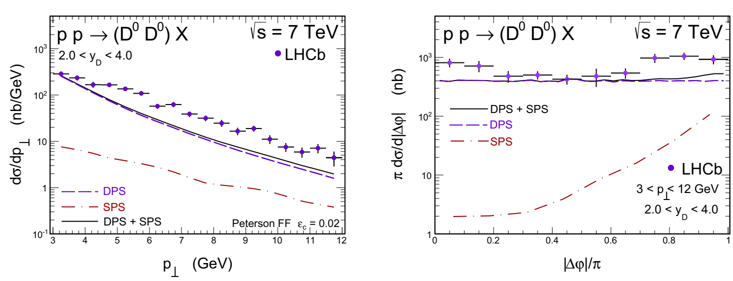

Figure 4. Distributions in meson transverse momentum when both mesons are measured within the LHCb acceptance and corresponding distribution in meson-meson azimuthal angle for DPS and SPS contributions.

In Fig. 4 we show distributions in meson transverse momentum (left panel) and meson-meson relative azimuthal angle (right panel). The shape in the transverse momentum is almost correct but some cross section is lacking. Similar situation is also observed in the case of the azimuthal angle distribution where the experimental data suggest some small correlations at small and large angles in contrast to the flat result of the standard DPS calculation. The SPS contribution (dash-dotted line) is compared to the DPS contribution (dashed line). The dominance of the DPS mechanism in description of the LHCb double charm data is clearly confirmed. The DPS mechanism gives a sensible explanation of the measured distribution, however some strength is still missing. This can be due to the single-ladder-splitting mechanisms discussed recently in Ref. [14].

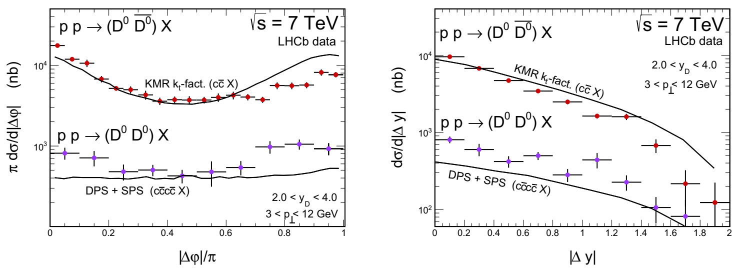

Figure 5. Azimuthal angle correlation between D^0D^0 and $D^0\bar{D}^0$ (left) and distribution in rapidity distance between two D^0 mesons and between $D^0\bar{D}^0$.

In Fig. 5 we compare correlations for D^0D^0 and $D^0\bar{D}^0$ in azimuthal angle (left panel) and in rapidity distance (right panel). The azimuthal angle distribution for identical mesons is somewhat flatter than that for $D^0\bar{D}^0$ which is consistent with the dominance of the DPS contribution. The rapidity distance distribution for $D^0\bar{D}^0$ falls down somewhat faster than in the case of identical D^0 mesons.

Recently, it has been found that there are (at least) two different types of contribution to the DPS cross section, which are accompanied by different geometrical prefactors (σ_{eff}'s) (see e.g. [16]). One of these is the standard conventional contribution in which two separate ladders emerge from both protons and interact in two separate hard interactions (see the left panel of Fig. 3). This is the one that is often considered in phenomenological analyses and has been applied in the studies presented above.

The other type of process is the perturbative single-ladder-splitting which is similar to the conventional mechanism except that one proton initially provides one ladder, which perturbatively splits into two (see the middle and right diagrams in Fig. 3).

Recently, the relative importance of the conventional and single-ladder-splitting DPS processes has been studied in Ref. [15], for various processes whose production is dominated by gluon-gluon fusion. In this study, the influence of the splitting contribution on the so-called effective cross section measured by comparison of the factorized model with experimental data has been carefully discussed.

In Fig. 6 we show transverse momentum (left panel) and rapidity (right panel) distribution of the charm quark/antiquark for the DPS mechanisms calculated within LO collinear approach at $\sqrt{s}$ = 7 TeV. The conventional and splitting terms are shown separately. The splitting contribution (lowest curve, red online) is smaller, but has almost the same shape as the conventional DPS contribution. The ratio of the DPS single-ladder splitting contribution to the conventional one in the case of double-charm production has been roughly estimated to be at the level of 30 – 60%. According to these results, the missing strengths in the description of the LHCb double charm data seem to be at least partially related to the parton splitting contribution.

The differential distributions in rapidity and in transverse momentum for the conventional and the parton-splitting contributions have essentially the same shape. This makes their model-independent separation extremely difficult. This also shows why the analyses performed are able to give reasonably good description of different experimental data sets only in terms of the conventional DPS contribution. The sum of the conventional and standard DPS contributions behaves almost exactly like the conventional contribution alone, albeit with a smaller σ_{eff} that depends only rather weakly on energy, scale and momentum fractions.

It is not clear in the moment how to combine the higher-order effects with the perturbative splitting mechanism. An interesting question is whether the ratio between the conventional and splitting contri-

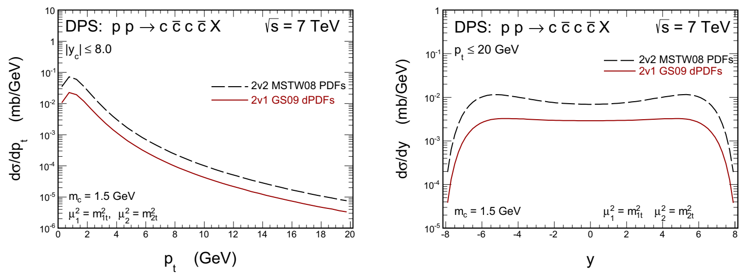

Figure 6. Transverse momentum (left panel) and rapidity (right panel) distribution of charm quark/antiquark for $\sqrt{s}$ = 7 TeV for conventional and single-ladder-splitting DPS mechanisms.

butions changes when higher-order corrections are included. Further studies in this context are clearly needed to fully include the splitting DPS contributions for the LHCb double charm experimental data.

Acknowledgements

This work was supported in part by the Polish grants DEC-2011/01/B/ST2/04535 and DEC-2013/09/D/ST2/03724 as well as by the Centre for Innovation and Transfer of Natural Sciences and Engineering Knowledge in Rzeszów.

References

[1] The ATLAS collaboration, ATLAS-CONF-2011-017.
[2] B.I. Abelev et al. (The ALICE collaboration), J. High Energy Phys. **01** (2012) 128.
[3] B.I. Abelev et al. (The ALICE collaboration), Phys. Lett. B **718**, 279 (2012).
[4] R. Aaij et al. (The LHCb collaboration), Nucl. Phys. B **871**, 1 (2013).
[5] R. Aaij et al. (The LHCb collaboration), J. High Energy Phys. **06**, 141 (2012).
[6] R. Maciuła and A. Szczurek, Phys. Rev. D **87**, 094022 (2013).
[7] M. Łuszczak, R. Maciuła, and A. Szczurek, Phys. Rev. D **85**, 094034 (2012).
[8] R. Maciuła, and A. Szczurek, Phys. Rev. D **87**, 074039 (2013).
[9] A. van Hameren, R. Maciula and A. Szczurek, Phys. Rev. D **89**, 094019 (2014).
[10] S. Catani, M. Ciafaloni and F. Hautmann, Nucl. Phys. B **366**, 135 (1991).
[11] C. Peterson, D. Schlatter, I. Schmitt, P.M. Zerwas, Phys. Rev. D **27**, 105 (1983).
[12] E. Lohrmann, arXiv:1112.3757 [hep-ex].
[13] M.A. Kimber, A.D. Martin and M.G. Ryskin, Phys. Rev. D **63**, 114027 (2001).
[14] J. R. Gaunt, J. High Energy Phys. **01** (2013) 042.
[15] J. R. Gaunt, R. Maciula and A. Szczurek, Phys. Rev. D **90**, 054017 (2014).
[16] J. R. Gaunt and W. J. Stirling, J. High Energy Phys. **03**, 005 (2010).